IEEE Access
Multidisciplinary | Rapid Review | Open Access Journal

Received 6 April 2023, accepted 19 April 2023, date of publication 24 April 2023, date of current version 27 April 2023.

Digital Object Identifier 10.1109/ACCESS.2023.3269575

RESEARCH ARTICLE

Active Fault Detection Based on Auxiliary Input Signal Design

JINGJING ZHANG[1], LIMING LIU[2], LEI WANG[1], AND FEIFAN YANG[3]
[1]School of Electrical Engineering, Hebei University of Architecture, Zhangjiakou 075000, China
[2]Sany Zhangjiakou Wind Power Technology Company Ltd., Zhangjiakou 075000, China
[3]School of Mechanical Engineering, Hebei University of Architecture, Zhangjiakou 075000, China

Corresponding author: Lei Wang (772813056@qq.com)

This work was supported by the Science and Technology Project of Hebei Education Department under Grant QN2022108.

ABSTRACT Active fault detection (AFD) is considered an effective incipient failure-detection method. In this paper, an auxiliary input resonance signal proposal that can detect different incipient faults quickly while keeping the system stable is proposed for AFD. To maintain the stability of the system, auxiliary input signals with a sinusoidal form, which should minimize and maximize the effect in fault-free cases and fault cases, are designed on the YJBK parameterization architecture. Subsequently, the fault detection signal is transferred from the traditional system output signal to the cumulative sum of the designed residual signal. Finally, some illustrative examples are given to indicate the effectiveness of the proposed unified operation architecture and some encourage results have been obtained, the simulation results show that the designed auxiliary input signal can not only ensure the normal operation of the system, but also quickly and effectively detect the occurrence of minor faults.

INDEX TERMS Active fault detection, auxiliary input signal, YJBK parameterization, unified operation architecture, resonance.

I. INTRODUCTION

Fault diagnosis has great significance to system reliability; therefore, to avoid accidents, increasingly complex industrial processes require more accurate and timely health monitoring and fault detection systems. A large number of approaches for initial minor faults have been presented in recent years [1], [2], [3], but most of these methods consider passive fault detection (PFD). The detector attempts to determine whether a failure has occurred only by monitoring the data of the system inputs and outputs. The PFD method is widely used for online real-time monitoring and is typically used in data-driven approaches, such as PCA, PLS, and SVM [4]. As a result of this, the initial minor faults are difficult to detect until they are disturbed or fully energized by the system reference input. To ensure system security, an active detection approach has been proposed in recent years. Active fault detection approach generally designs a test signal to detect abnormal behaviors that would otherwise remain undetected because the system would remain stable and operate normally during a faulty period [5], [6], [7]. Compared with PFD, active fault detection (AFD) can provide much faster detection of small faults and is mainly applied to closed-loop systems [8]. The active approach requires that an auxiliary signal be applied to the system for fault detection, and a cost function is used to optimize the test signal, which does not disturb the detected system as much as possible.

To realize active fault detection process, Niemann et al. proposed unique AFD solutions for parameter faults [9], MIMO systems [10] and sampled-data systems. The idea of injecting a signal into the system is to determine the values of the various physical parameters. However, additional input signals have been introduced in the context of fault detection and developed later. Their approach focused on the design of a fixed random auxiliary signal. A general AFD scheme was presented by Puncachaf and Simandl [11], [12]. They focused on setting up a unified formulation of the AFD and system control (AFDC). Subsequently, three special AFD cases are proposed, which are combined by a signal generator, fault detector, and system controller [13], [14], [15].

The associate editor coordinating the review of this manuscript and approving it for publication was Baoping Cai.

Nikoukhah and Campbell et al. presented a novel AFD approach based on a mathematical view, and the solutions were based on control theories. Several research results have been proposed, such as auxiliary signal design and incipient fault detection [16], [17], [18], [19], [20], [21], [22]. Jing et.al. proposed a unified architecture for active fault detection and partial active fault-tolerant control of incipient faults [1], [23].

The above research methods and content for the detection of minor problems are of great significance; however, the design process is relatively complex, and the design of the auxiliary signal or the design of the excitation signal generator is more relevant to the system. In this study, the auxiliary input signal was designed directly and then injected into the system, which has a clear and concise design objective. The architecture of the system was constructed using the Youla parameter [15] and the decision signal was designed based on it. We first analyzed the relationship between the fault signature matrix and the parameter fault and frequency, which illustrates why the design signal is sinusoidal. Then, according to the design requirements, a proper cost function can be designed to find the optimized frequency and amplitude of the auxiliary input signal, and the multi-objective optimization method is used. The design idea of the frequency is based on the thought of random resonance of minor fault detection [24], [25], [26], [27], but in our research method, the frequency is designed as a fixed value in connection with a certain type and size fault. Therefore, we designed a series of auxiliary input signals with a certain frequency for each type of faulty system and then combined them to inject a system with an unknown fault to detect whether the fault occurs or not.

Different from the traditional fault detection methods which are mostly data-driven, the proposed sinusoidal auxiliary input signal method plays an active role in minor fault detection. This method does not need to conduct fault location monitoring after fault alarm, but can quickly and effectively detect hidden faults while ensuring the safe and stable operation of the system when minor faults occur and the system is still within the range of safe operation threshold, providing a reliable technical route for safe production. The design of AFD satisfies two requirements.

1) The closed-loop system is stable when it is in normal operation condition.

2) When incipient parameter fault occurs, system output residuals caused by minor fault will increase greatly even to unstable status.

The remainder of this paper is organized as follows. The problem formulation and system architecture are described in section II. Section III explains the fault decision signal design and the main concept of designing auxiliary signals for active fault detection. Finally, the simulations are presented in Section IV, and conclusions are drawn in Section V.

II. PROBLEM FORMULATION

In this study, a parameter fault is considered to be a signal that causes the system to be abnormal. The parameter fault type is described by changing the parameters of the state-space model. In this section, some fundamental problems related to YJBK parameterization [15] are briefly discussed. These materials are frequently used in the remainder of this study.

Considering the system state space description as:

$$\begin{cases} \dot{x} = Ax + Bu + B_d d + B_w w \\ z = C_z x + D_{zu} u + D_{zd} d + D_{zw} w \\ y = C_y x + D_{yu} u + D_{yd} d + D_{yw} w \end{cases} \tag{1}$$

and the system transfer function can be written as:

$$\begin{aligned} z(s) &= (C_z (SI - A)^{-1} B + D_{zu}) u(s) + (C_z (SI - A)^{-1} B_d \\ &\quad + D_{zd}) d(s) + (C_z (SI - A)^{-1} B_w + D_{zw}) w(s) \\ &= G_{zu} u(s) + G_{zd} d(s) + G_{zw} w(s) \\ y(s) &= (C_y (SI - A)^{-1} B + D_{yu}) u(s) + (C_y (SI - A)^{-1} B_d \\ &\quad + D_{yd}) d(s) + (C_y (SI - A)^{-1} B_w + D_{yw}) w(s) \\ &= G_{yu} u(s) + G_{yd} d(s) + G_{yw} w(s) \end{aligned} \tag{2}$$

where $u \in R_u^m$, $x \in R_x^m$, $y \in R_y^m$, and $d \in R_d^m$ are the control input signal, state vector, measurement output vector, and external disturbance, respectively, and $d \in R_d^m$ represents a series of disturbances $\{d_1, d_2, \ldots\ldots d_n\}$ that may occur at any location. The signals $w \in R_w^m$ and $z \in R_z^m$ are the external input vector and output vector, respectively.

In this paper, Δ represents the parameter fault in the system, and only minor parameter faults are considered, i.e. $\delta_0 < |\Delta| < \delta_1 \ll 1$ (where δ_0 and δ_1 are two given slight positive number, such as $\delta_0 = 0.01$ and $\delta_1 = 0.1$). When there is no noise in the system, that is, $d = 0$, the traditional feedback control system can be described as a linear fractional transformation (LFT) using the H_∞ optimal method, as shown in Fig.1 [1].

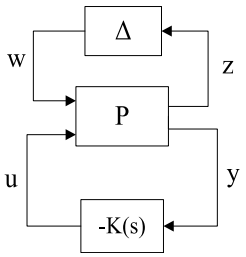

FIGURE 1. LFT form of the feedback system.

where $P = \begin{pmatrix} G_{zw} & G_{zu} \\ G_{yw} & G_{yu} \end{pmatrix}$ and $K(s)$ represent the stable feedback controllers. Parameter fault Δ is an unknown constant; when multiple faults occur, the fault can be described as Δ_i $(i = 1, 2, \ldots, k)$. To elaborate on the research emphasis, we considered only one fault that occurred. Therefore, the faulty system can be described by changing the transfer function parameter with fault Δ, as shown in Table. In this study, the parameter faulty system is described as $G_{yu}(\Delta)$.

The system $G_{yu}(s) = C_y (SI - A)^{-1} B + D_{yu}$ from (3) and a stable controller $K(s)$ [15] can be obtained through

coprime factorization.

$$\begin{cases} G_{yu}(s) = NM^{-1} = \tilde{M}^{-1} = \tilde{M}^{-1}\tilde{N} & N, M, \tilde{M}, \tilde{N} \in RH_\infty \\ UV^{-1} = \tilde{V}^{-1}\tilde{U} = K(s) & U, V, \tilde{U}, \tilde{V} \in RH_\infty \end{cases} \tag{3}$$

The feedback controller $K(s)$ is designed based on H_∞ algorithm to ensure system stability, and the $N, M, \tilde{N}, \tilde{M}, U, V, \tilde{U}, \tilde{V}$ informula (4) must satisfy the double Bezout equation:

$$\begin{aligned} \begin{pmatrix} I & 0 \\ 0 & I \end{pmatrix} &= \begin{pmatrix} \tilde{V} & -\tilde{U} \\ -\tilde{N} & \tilde{M} \end{pmatrix} \begin{pmatrix} M & U \\ N & V \end{pmatrix} \\ &= \begin{pmatrix} M & U \\ N & V \end{pmatrix} \begin{pmatrix} \tilde{V} & -\tilde{U} \\ -\tilde{N} & \tilde{M} \end{pmatrix} \end{aligned} \tag{4}$$

According to Fig. 2 in [1], $G_{yu}(s)$ represents the transfer function of the system (1). $K(s)$ denotes the feedback controller. After the coprime factorization for the system $G_{yu}(s)$ and the controller reconfiguration and ignoring the external noises, the closed-loop system block diagram is shown in Fig. 2 [9].

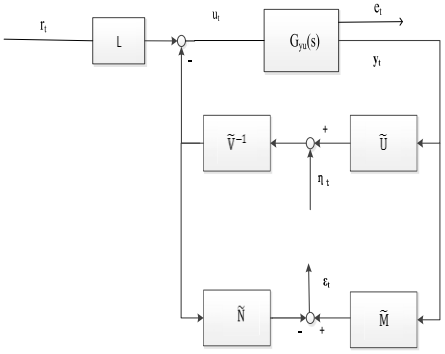

FIGURE 2. AFD based on auxiliary input signal design.

Signal e_t is the residual output. The proper gain L must be designed such that the system output y_t tracks the reference signal r_t. Signal η_t in Fig.2 is the auxiliary input signal that we designed. Thus, it is easy to obtain the system output.

$$y_t = \left(r_t L - \tilde{V}^{-1}\left(\tilde{U}y_i + \eta_t\right)\right) G_{yu}(s) \tag{5}$$

$$\varepsilon_t = \tilde{M}y_t - \tilde{N}\left(\left(\tilde{U}y_t + \eta_t\right)\tilde{V}^{-1}\right) \tag{6}$$

Substitute (7) into (6), it is obtained:

$$e_t = y_t = \frac{r_t L G_{yu}(s) - \tilde{V}^{-1}\eta_t G_{yu}(s)}{1 + \tilde{V}^{-1}\tilde{U}G_{yu}(s)} \tag{7}$$

The described contents of the above problems have used the eight matrixes $N, M, \tilde{N}, \tilde{M}, U, V, \tilde{U}, \tilde{V}$. These eight stable matrices for configuring the controlled system G_{yu}(s) and feedback controller $K(s)$ were calculated according to the following equations:

$$\begin{pmatrix} M & V \\ N & U \end{pmatrix} = \left(\begin{array}{c|cc} A+BF & B & H \\ \hline F & I & 0 \\ C_F & D & I \end{array}\right) \tag{8}$$

$$\begin{pmatrix} \tilde{V} & -\tilde{U} \\ -\tilde{N} & \tilde{M} \end{pmatrix} = \left(\begin{array}{c|cc} A-HC & -B_H & -H \\ \hline F & I & 0 \\ C & -D & I \end{array}\right) \tag{9}$$

with $C_F = C + DF$ and $B_H = B - HD$. Here, F and H are the feedback gain matrix and observer gain such that $AF = A+BF$ and $AH = A-HC$ are Hurwitz matrices, respectively.

A. THE SYSTEM SET UP

In order to simplify the system description, let the general system be given by

$$\sum P, \Delta : \begin{cases} e_t = G_{er}(\Delta)r_t + G_{eu}(\Delta)u_t \\ y_t = G_{yr}(\Delta)r_t + G_{yu}(\Delta)u_t \end{cases} \tag{10}$$

The system is set up in Fig.1, and based on it, the signal u_t is given by:

$$u_t = (y_t\tilde{U} + \eta_t)\tilde{V}^{-1} \tag{11}$$

When external noise is ignored, the system can be regarded as a two-input, two-output system, as shown in Fig.3.

FIGURE 3. System set up for active fault diagnosis.

The transfer functions from the two inputs r_t, η_t to the two outputs ε_t, e_t are given by

$$\sum FD : \begin{cases} e_t = P_{er}(\Delta)r_t + P_{e\eta}(\Delta)\eta_t \\ \varepsilon_t = P_{\varepsilon r}(\Delta)r_t + P_{\varepsilon\eta}(\Delta)\eta_t \end{cases} \tag{12}$$

and we can get that

$$P_{er}(\Delta) = G_{er}(\Delta) + \frac{G_{eu}(\Delta)\tilde{U}G_{yr}(\Delta)}{\tilde{V} - G_{yu}(\Delta)\tilde{U}} \tag{13}$$

$$P_{e\eta}(\Delta) = \frac{G_{eu}(\Delta)}{\tilde{V} - G_{yu}(\Delta)\tilde{U}} \tag{14}$$

$$P_{\varepsilon r}(\Delta) = \frac{G_{yr}(\Delta)}{\tilde{V} - G_{yu}(\Delta)\tilde{U}} \tag{15}$$

$$P_{\varepsilon\eta}(\Delta) = -\frac{\tilde{N} - G_{yu}(\Delta)\tilde{M}}{\tilde{V} - G_{yu}(\Delta)\tilde{U}} \tag{16}$$

In early research, a stable dual YJBK parameter S_f which is also called a fault signature matrix in connection with parametric faults for the controlled system G_{yu}(s) with faults, is denoted as G_f(s), that is,

$$G_f(s) = G_{yu}(S_f) = (N + VS_f)(M + US_f)^{-1} \tag{17}$$

or

$$G_{yu}(S_f) = (\tilde{M} + S_f U)^{-1}(\tilde{N} + S_f\tilde{V}) \tag{18}$$

The dual YJBK transfer function S_f is calculated by

$$\begin{aligned} S_f &= (G_f(s)M - N)(V - G_f(s)U)^{-1} \\ &= (\tilde{V} - \tilde{U}G_f(s))^{-1}(\tilde{M}G_f(s) - \tilde{N}) \end{aligned} \tag{19}$$

In previous studies, the parameter S_f was calculated for different faulty types. The different faulty type systems and the dual YJBK parameter S_f for a few typical parametric faults Δ are listed in Table. 1 [1].

TABLE 1. Typical parameter faults Δ and dual YJBK parameter.

$G_f(s) = G_{yu}(\Delta)$	$S_f(\Delta)$
G_{yu}	0
$(I+\Delta)G_{yu}$	$\tilde{M}\Delta(I - N\tilde{U}\Delta)^{-1}N$
$G_{yu}(I+\Delta)$	$\tilde{N}\Delta(I - U\tilde{N}\Delta)^{-1}M$
$G_{yu}+\Delta$	$\tilde{M}\Delta(I - U\tilde{M}\Delta)^{-1}M$
$G_{yu}(I+\Delta)^{-1}$	$-\tilde{N}\Delta(I + M\tilde{V}\Delta)^{-1}M$
$(I+\Delta)^{-1}G_{yu}$	$-\tilde{M}\Delta(I + V\tilde{M}\Delta)^{-1}N$
$G_{yu}(I+\Delta G_{yu})^{-1}$	$-\tilde{N}\Delta(I + N\tilde{V}\Delta)^{-1}N$
$(N+\Delta_N)(M+\Delta_M)^{-1}$	$(-\tilde{N}\tilde{M})\begin{pmatrix}\Delta_M \\ \Delta_N\end{pmatrix}(I+(V-U)\begin{pmatrix}\Delta_M \\ \Delta_N\end{pmatrix})^{-1}$
$(\tilde{M}+\Delta_{\tilde{M}})^{-1}(\tilde{N}+\Delta_{\tilde{N}})$	$\left(I+(\Delta_{\tilde{M}}\ \Delta_{\tilde{N}})\begin{pmatrix}\tilde{V} \\ -\tilde{U}\end{pmatrix}\right)^{-1}(\Delta_{\tilde{M}}\ \Delta_{\tilde{N}})\begin{pmatrix}-N \\ M\end{pmatrix}$

where Δ represents different parameter faults occurring in different parts of the controlled system; Δ_M, Δ_N, $\Delta_{\tilde{M}}$ and $\Delta_{\tilde{N}}$ are the corresponding parameter faults occurring in the coprime factorization matrices $M, N, \tilde{M}, \tilde{N}$, respectively.

ΣFD of the system Σ_{FD} is shown in Fig.3. The transfer function from the input signal η_t to the residual ε_t is equal to the dual YJBK transfer function S_f [23]. An important aspect of this connection is that the dual YJBK transfer function is zero in the nominal case. This implies that the transfer function from the auxiliary input η_t to the residual ε_t is zero in the nominal case. Therefore, when a fault occurs, the dual YJBK transfer function S_f will have an effect on the system, and we can analyze S_f to look for a breakthrough in fault detection.

B. THE RELATIONSHIP BETWEEN THE PARAMETER S_f AND FREQUENCY w

When faults occur, the transfer function $G_f(s)$ (i.e., $G_{yu}(\Delta)$) of the faulty system can be described by the parameter S_f and fault Δ. And the relationship between them has been discussed in paper [1], and S_f can be seen as a transfer function in the above expression, then for the transfer function, it can be analyzed in the amplitude-frequency characteristics. Thus, parameter S_f may be related to the design of the frequency of the auxiliary signal. Therefore, what is the relationship between S_f and the frequency w? In this subsection, the dual YJBK parameters, S_f and w are discussed in detail.

According to prior knowledge, the parameter fault Δ may have an inner relationship with the dual YJBK parameter S_f. To provide a more theoretical analysis to find this relationship, we are trying to do so. If the location and type of the fault are completely different, the corresponding parameter S_f has a different expression and formula definition, as listed in Table. 1. To determine the general connection between fault Δ and the dual YJBK parameter S_f, we chose a generic type of fault to complete a detailed inner relationship analysis. Suppose that the parameter fault description is

$$G_{yu}(\Delta) = G_{yu}(I + \Delta) \tag{20}$$

The corresponding dual YJBK parameter $S_f(\Delta)$ is

$$S_f(\Delta) = \tilde{N}\Delta\left(I - U\tilde{N}\Delta\right)^{-1}M \tag{21}$$

$S_f(\Delta)$ is a plural function; therefore, only the amplitude-frequency characteristic can be analyzed. In particular, the relationship between the amplitude of $S_f(\Delta)$ and frequency ω was analyzed. We use an example to illustrate this relationship. Assumption

$$S_f(\Delta) = \frac{(s+1)\Delta}{\left(s^2 + 5s + 6\right) + 2\Delta} \tag{22}$$

For a fixed Δ, the partial derivative of $log_{10}|S_f(w, \Delta)|$ along with w and the simulation of the relationship can be described as shown in Fig.4.

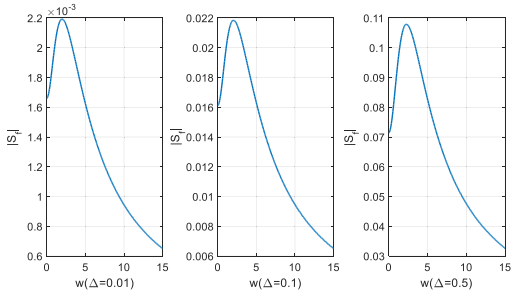

FIGURE 4. |Sf (w, Δ)| along to w.

For the same fault Δ,

(1) When frequency $0 < w < w_1$, $\lg|S_f|$ monotonically increases with an increase in frequency w, and the monotone is significant.
(2) When frequency $w_1 < w < w_2$, the amplitude of $\lg|S_f|$ increases sequentially, but the increasing monotone becomes less significant. Then, the partial derivative of $log_{10}|S_f\ (w, \Delta)|$ is reduced. Therefore, the amplitude of the partial derivative of $log_{10}|S_f\ (w, \Delta)|$ may have a maximum value in this region.
(3) When the frequency $w > w_2$, $\lg|S_f|$ monotonically decreases with increasing frequency w.

The fault signature matrix is a measure of the effect of parameter variation on closed-loop stability. The above analysis of S_f indicates that the parameter variations have a major influence on the system. Therefore, parameter S_f may be related to the design of the frequency of the auxiliary signal.

C. THE FORM OF AUXILIARY INPUT SIGNAL

In addition to the above-mentioned methods of minor fault detection, resonance-assisted signal methods have also been proposed, such as random resonance. In contrast to traditional noise, the random resonance phenomenon reflects the positive effect of noise in terms of fault detection. This idea has been applied in many fields, in which the detection of small signals is a typical application. This provides new ideas and prospects for the detection of minor fault signals. However, when random resonance is used to detect a minor signal, the required frequency range is not conducive for rapid detection. This idea is further innovative in this study. The excitation signal is designed as a sinusoidal signal form, which has a fixed frequency, and will help the system detect known types and sizes of faults quickly.

The auxiliary signal η is designed to be a sinusoidal curve in this study, and its expression can be written as

$$\eta = \lambda \sin(\omega t) \tag{23}$$

The design target is to find the appropriate amplitude λ and frequency ω. Because the actual failure is unknown, an auxiliary signal designed for a single fault type may not detect all types of faults. Therefore, we designed excitation signals for each type of fault, and the composition of the integrated signal was used for unknown fault detection. The form of the new integrated excitation signal is $\eta = \eta_1 + \eta_2 + \eta_3 + \eta_4 + \ldots$

III. ACTIVE FAULT DETECTION BASED ON AUXILIARY INPUT SIGNAL DESIGN

A. THE DETECTION DECISION DESIGN

In this research method, because it involves the problem of maintaining the stability of the system, fault detection needs to redesign the fault indicator to judge whether the fault has occurred. For some methods, the active fault detection method based on controller reconfiguration is based on the system output offset to determine the decision signal of fault occurrence. However, in a method based on auxiliary input signal design, the system remains stable after a failure; therefore, we need to design a decision signal that can detect the fault quickly.

In the above research, we propose the basic framework of the study. Based on this, an auxiliary input signal injection location was designed. Then, the relationship between the fault feature matrix S_f and frequency ω is analyzed, and the system has the characteristics of natural frequency. Therefore, to compensate for the shortcomings of the speed in detecting small signals with resonant low-frequency scanning, a sinusoidal excitation signal with a fixed frequency was proposed. In AFD, the design goal is to ensure system stability while detecting the fault, and the system stability criterion is the system output and the system residual. Here, we use the residual as the basis for fault decision signal design, and the cumulative sum (CUSUM) method is adopted. The cumulative signal can be written as [23]

$$\delta = \left| \int_0^T \varepsilon_t e^{jwt} d_t \right| \tag{24}$$

When the residual ε_t of the faulty system is beyond a certain range of the nominal system residual, the cumulative signal is calculated.

According to the design form of this signal, in the following design scheme, the signal is regarded as a known quantity, and the specific amplitude and frequency of the auxiliary input signal are calculated in detail.

B. THE FREQUENCY W DESIGN OF AUXILIARY SIGNAL

The purpose of detection is to detect the imperceptible parameter failure of the system. Meanwhile, we also hope that the system under normal circumstances will not be destroyed by the auxiliary input signal. Therefore, the auxiliary input signal η must be designed with respect to:

- The effect of the auxiliary input signal η on the external output e in the fault-free case is minimized.

$$\min |P_{e\eta}(0)| \tag{25}$$

- The signature from the auxiliary input signal η is maximized to the residual ε in the fault case.

$$\max |P_{\varepsilon\eta}(\Delta)| \Rightarrow \max |S_f(\Delta)| \tag{26}$$

Then the performance indicators can be written as

$$J_\omega = \frac{\alpha |S_f(\Delta)|}{(1-\alpha)|P_{e\eta}(0)|} \tag{27}$$

The design goal is to maximize the cost function, and then the frequency and amplitude of the auxiliary input signal can be designed according to Eq. (24).

$$\max J_\omega = \max \frac{\alpha |S_f(\Delta)|}{(1-\alpha)|P_{e\eta}(0)|} \tag{28}$$

Through the above content, we will select a specific example to solve the objective function, and then obtain the frequency w. Using the fault type $G_{yu}(\Delta) = (I + \Delta)G_{yu}$ as an example, we can obtain

$$P_{\varepsilon\eta}(\Delta) = S_f = \tilde{N}\Delta(I - U\tilde{N}\Delta)^{-1}M \tag{29}$$

$$|P_{e\eta}(0)| = \left|\frac{NM^{-1}}{V - NM^{-1}U}\right| = \left|\frac{N}{VM - NU}\right| \tag{30}$$

so the objective function can be rewritten as

$$\max J_\omega = \max\left(\frac{\alpha|\tilde{N}\Delta(I - U\tilde{N}\Delta)^{-1}M|}{(1-\alpha)\left|\frac{N}{VM-NU}\right|}\right) \tag{31}$$

The fault signature matrix in connection with the AFD is a transfer function. Hereafter, it is denoted by S_f, where $S_f = P_{\varepsilon\eta}(\Delta)$. An explicit equation for S_f was derived in [9].

By determining the relationship between the fault feature matrix and frequency according to Table. 1, we convert the problem of fault detection to a frequencylevel to solve. The objective function can be rewritten as formula (33), and the following sections describe the specific design method and provide simulations to illustrate it.

$$\omega = \arg\max_{\omega}\left(\frac{\alpha|\tilde{N}\Delta(I-U\tilde{N}\Delta)^{-1}M|}{(1-\alpha)|\frac{N}{VM-NU}|}\right) \tag{32}$$

Here, we regard the auxiliary input signal and performance indicators as a virtual closed-loop system and then optimize the auxiliary input signal frequency continuously through the performance indicators, as shown in Fig.5.

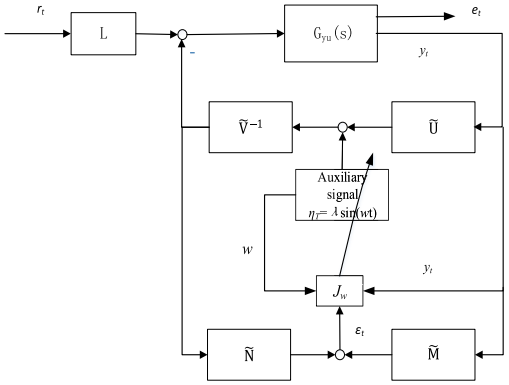

FIGURE 5. Optimization of performance indicators with the Youla parameterization structure.

By optimizing the frequency of the performance index with the specific fault size, a series of optimal frequencies can be obtained in the fault size definition domain, The specific optimization form is shown in formula (32)

$$\omega_{k+1} = \omega_k + \alpha'\frac{\partial|J_\omega|}{\partial\omega} \tag{33}$$

The auxiliary input signal amplitude in this chapter is also an important parameter design, which introduces the design methods and ideas of the amplitude.

Remark 1: In this study, the design of the excitation signal was inspired by the idea of random resonance. The auxiliary signal form was designed as a sinusoidal signal, and the frequency was designed based on resonance ideas. In previous research results, many studies using random resonance were thought to detect weak signals, and the required frequency range was not conducive to the rapid detection of small signals. Therefore, to compensate for the shortcomings of detection speed, this study further innovates this idea. The excitation signals were designed as sinusoidal signals with a fixed frequency, which improved the detection. The overall design framework is a closed-loop structure, and the fault decision signal is closely related to the design of the auxiliary input signal, reflecting the idea of "active."

C. THE AMPLITUDE DESIGN OF AUXILIARY SIGNAL

The purpose of active fault detection is to detect imperceptible failures under the premise that the system is stable. Then, we set the desired output size as H (system quality), set the system output upper bound threshold as $H+\Delta H_1$, and set the system output upper bound threshold range to $H+\Delta H_2$ (engineering safety range), as shown in Fig.6.

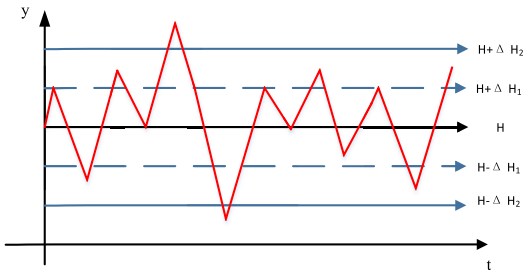

FIGURE 6. The desired system output and the thresholds.

Earlier we have obtained the relationship between the auxiliary input signal and the output:

$$\sum FD: \begin{cases} e_t = P_{er}(\Delta)r_t + P_{e\eta}(\Delta)\eta_t \\ \varepsilon_t = P_{\varepsilon r}(\Delta)r_t + P_{\varepsilon\eta}(\Delta)\eta_t \end{cases} \tag{34}$$

In the fault-free case, the component of the auxiliary input signal in the output is

$$P_{e\eta}(0)\eta_t \tag{35}$$

The form of the final decision signal is illustrated by means of the accumulated signal

$$\delta = \pm\left|\int_0^T \varepsilon_t e^{jwt}d_t\right| \tag{36}$$

where

$$\varepsilon_t = My_t - N(r_tL - u_t) \tag{37}$$

To detect faults as accurately as possible, it is possible to specify that td is the minimum detection time; that is, if the residual signal is not always in the abnormal range during the minimum detection time, the accumulated signal will be reset to zero and continues to the next stage of accumulation; if the residual signal is abnormal all the time, then the accumulation of this stage continues, and it is desirable to detect the fault within the minimum detection time. The cumulative lower limit is set to χ, considering the occurrence of the fault, that is, the residual has been in a small abnormal state (regardless of external interference, the residual normal state should be 0), and the detection limit can be set as

$$\begin{aligned} \delta &= \left|\int_0^{t_d} \varepsilon_t e^{jwt}d_t\right| \geq \chi \\ &\Rightarrow \left|\int_0^{t_d} |(\tilde{M}y_t - \tilde{N}(r_tL - u_t))|e^{jwt}d_t\right| \geq \chi \\ &\Rightarrow \left|\int_0^{t_d} (|\frac{\tilde{M}G_{eu}(\Delta) - \tilde{N}}{\tilde{V} - G_{yu}(\Delta)\tilde{U}}|\lambda\sin(\omega t))e^{jwt}d_t\right| \geq \chi \end{aligned} \tag{38}$$

where

$$\chi = \delta\%H \tag{39}$$

where $\delta\%$ is a percentage of engineering significance to the system. To ensure system stability when detecting faults, the component of the auxiliary input signal in the output should have an upper limit, which is the desired fluctuation range threshold $H + \Delta H_1$ in this study, and one of the constraints can be obtained as

$$\begin{aligned} |P_{e\eta}(0)\eta_t| \ &\leq \ |\Delta H_1| \\ &\Rightarrow |\frac{G_{yu}(0)}{V - G_{yu}(0)U}\lambda \sin(\omega t_d)| \leq |\Delta H_1| \end{aligned} \tag{40}$$

so the design object can be written as

$$\begin{aligned} &\min \lambda \\ &st. \begin{cases} P_{e\eta}(0)\eta_t < |\Delta H_1| \\ \delta = \left| \int_0^{t_d} \varepsilon_t e^{jwt} d_t \right| \geq \chi \end{cases} \end{aligned} \tag{41}$$

Then the cost function of designing the amplitude is

$$J_\lambda = \lambda + \beta_1(P_{e\eta}(0)\eta_t - |\Delta H_1|) + \beta_2(\chi - \delta) \tag{42}$$

where β_1 and β_2 are relaxation factors, and minimizing the cost function can be the design idea of the amplitude, which is set as (41). Similarly, using the gradient algorithm, the calculated amplitude can be expressed as Eq.(43),

$$\min J_\lambda \tag{43}$$

$$\lambda_{k+1} = \lambda_k + \frac{\partial J(\lambda)}{\partial \lambda} \tag{44}$$

According to the above design method for amplitude and frequency, we can obtain the desired auxiliary input signal:

$$\eta = \lambda^* \sin(\omega^* t) \tag{45}$$

where λ^* and ω^* are certain values of the amplitude and frequency of the auxiliary input signal, respectively. Subsequently, the auxiliary input signal can be injected into the system, and the final effect of the design is verified in the simulation section.

The calculation process of this paper is complicated, and the meanings of the calculated letters and symbols are summarized in Table. 2.

IV. CASE ANALYSIS AND SIMULATION

In this section, the frequency and amplitude of the auxiliary input signal are calculated using a practical case, and simulations are performed to describe the work of AFD.

A. AUXILIARY SIGNAL FREQUENCY W CALCULATION

To better illustrate the design of this method, as well as a more intuitive observation of the calculation process and ideas, a simple first-order system is chosen as an example:

$$G(s) = \frac{c}{as + b} \tag{46}$$

TABLE 2. The symbolic meaning.

Symbol	Symbolic meaning
δ	the accumulated signal
ε_t	Residual error
χ	The cumulative lower limit
H	the desired output size
$H + \Delta H_1$	the system output upper bound threshold

The state space of the system can be expressed as

$$\begin{aligned} \dot{x} &= Ax + Bu \\ y &= Cx + Du \end{aligned} \tag{47}$$

where

$$A = -\frac{b}{a}, \quad B = 1, \ C = \frac{c}{a}, \ D = 0$$

The expressions of the system and system controller can be obtained using the Youla parameter, and the state feedback and output feedback poles are set as m and n, respectively. Then we have

$$\begin{aligned} A_F &= A + BF, \quad A_H = A + HC \\ C_F &= C + DF, \quad B_H = B + HD \end{aligned} \tag{48}$$

where

$$\begin{aligned} F &= m + \frac{b}{a}, \quad H = \frac{an + b}{c} \\ C_F &= \frac{c}{a}, \quad B_H = 1 \end{aligned}$$

according to formula (9)(10),we can obtain that

$$\begin{aligned} M(s) &= \frac{as + b}{a(s - m)}, N(s) = \frac{c}{a(s - m)} \\ V(s) &= \frac{as - b - a(m + n)}{a(s - m)} \\ U(s) &= \frac{-(am + b)(an + b)}{ac(s - m)} \end{aligned} \tag{49}$$

$$\begin{aligned} \tilde{M}(s) &= \frac{as + b}{a(s - n)}, \tilde{N}(s) = \frac{c}{a(s - n)} \\ \tilde{V}(s) &= \frac{as - b - a(m + n)}{a(s - n)} \\ \tilde{U}(s) &= \frac{-(am + b)(an + b)}{ac(s - n)} \end{aligned} \tag{50}$$

By selecting the faulty type as $G_{yu}(\Delta) = G_{yu}(I + \Delta)$, the transfer function of the auxiliary input signal η to the external output e in the fault-free case and to the residual ε in the fault case can be obtained as:

$$|P_{e\eta}(0)| = |\frac{NM^{-1}}{V - NM^{-1}U}| = |\frac{N}{VM - NU}|$$

$$= |\frac{c}{a(s-n)}| = |\frac{c}{a(wj-n)}|$$
$$= \frac{|c|}{|a|\sqrt{w^2+n^2}} \tag{51}$$

when fault occurs,

$$\begin{aligned}
&|P_{\varepsilon\eta}(\Delta)| \\
&= |S_f| = |\tilde{N}\Delta(I - U\tilde{N}\Delta)^{-1}M| \\
&= |\frac{ac(as+b)\Delta}{a^2(s-m)(s-n)+(am+b)(an+b)\Delta}| \\
&= |\frac{ac\Delta(awj+b)}{a^2(mn-w^2)+(am+b)(an+b)\Delta - a^2(m+n)wj}| \\
&= \frac{|ac\Delta|\sqrt{a^2w^2+b^2}}{\sqrt{[a^2(mn-w^2)+(am+b)(an+b)\Delta]^2+(a^2(m+n)w)^2}}
\end{aligned} \tag{52}$$

According to them, the objective function to be optimized can be written as

$$\begin{aligned}
&\frac{|P_{\varepsilon\eta}(\Delta)|}{|P_{e\eta}(0)|} \\
&= \frac{|a\Delta|\sqrt{a^2w^2+b^2}\sqrt{a^2w^2+a^2n^2}}{\sqrt{[a^2(mn-w^2)+(am+b)(an+b)\Delta]^2+(a^2(m+n)w)^2}}
\end{aligned} \tag{53}$$

To obtain the maximum value, we must use the extreme value theorem to find the derivative with frequency, and the partial derivative of the objective function with respect to frequency is obtained:

$$\begin{aligned}
\frac{\partial \frac{|S_f(\Delta)|}{|P_{e\eta}(0)|}}{\partial w} &= \frac{\partial \frac{|a\Delta|\sqrt{a^2w^2+b^2}\sqrt{a^2w^2+a^2n^2}}{\sqrt{[a^2(mn-w^2)+(am+b)(an+b)\Delta]^2+(a^2(m+n)w)^2}}}{\partial w} \\
&= |a\Delta|\frac{A}{B}
\end{aligned} \tag{54}$$

where

$$\begin{aligned}
A = {} & w^5[a^8(m^2+n^2) - a^4(a^4n^2+a^2b^2) \\
& - 2a^6(am+b)(an+b)\Delta] \\
& + w^3[4a^6mn(am+b)(an+b)\Delta \\
& + 2a^4(am+b)^2(an+b)^2\Delta^2 \\
& + 2a^8m^2n^2 - 2a^6b^2n^2] \\
& + w[(a^4n^2+a^2b^2)[(am+b)(an+b)\Delta + a^2mn]^2 \\
& - a^6b^2n^2(m^2+n^2) + 2a^4b^2n^2(am+b)(an+b)\Delta] \\
B = {} & [(a^2(mn-w^2)+(am+b)(an+b)\Delta)^2 \\
& + a^4(m+n)^2w^2]^{1.5} \\
& \times \sqrt{a^4w^4+(a^4n^2+a^2b^2)w^2+a^2b^2n^2}
\end{aligned}$$

Then the specific optimization form is rewritten as

$$\begin{aligned}
\omega_{k+1} &= \omega_k + \alpha\frac{\partial|J_\omega|}{\partial\omega} \\
&= \omega_k + \alpha'\frac{\alpha}{1-\alpha}|a\Delta|\frac{A}{B}
\end{aligned} \tag{55}$$

We have designed the auxiliary input signal above, and in this section, some simulations are shown. To illustrate the feasibility of the method, we select a general signal input–output system as an example:

$$G(s) = \frac{1}{s+1}$$

that is, the parameter in (51) is selected as $a = -1$, $b = 1$, $c = 1$, and the faulty type is selected as

$$G_f(\Delta) = \frac{1(1+\Delta)}{s+1}$$

Here, we take an active fault detection process for this faulty type. First, the frequency and amplitude of the auxiliary input signal are calculated according to the above method; the system closed-loop poles are set as $m = -3$, $n = -4$, and then we can obtain

$$\begin{aligned}
M(s) &= \frac{s+1}{s+3}, \quad N(s) = \frac{1}{s+3}, \\
V(s) &= \frac{s+6}{s+3}, \quad U(s) = \frac{-6}{s+3} \\
\tilde{M}(s) &= \frac{s+1}{s+4}, \quad \tilde{N}(s) = \frac{1}{s+4}, \\
\tilde{V}(s) &= \frac{s+6}{s+4}, \quad \tilde{U}(s) = \frac{-6}{s+4}
\end{aligned}$$

So the objective function can be rewritten as

$$\begin{aligned}
\omega &= \arg\max_{\omega}(\frac{\alpha|\tilde{N}\Delta(I-U\tilde{N}\Delta)^{-1}M|}{(1-\alpha)|\frac{N}{VM-NU}|}) \\
&= \arg\max_{\omega}(\frac{\alpha}{(1-\alpha)}|\frac{(s+1)(s+4)\Delta}{(s+3)(s+4)+6\Delta}|)
\end{aligned}$$

Let

$$Q = |\frac{(s+1)(s+4)\Delta}{(s+3)(s+4)+6\Delta}|$$

To obtain the value of the frequency w when the cost function Q is maximum, set $s = jw$ and transfer the problem to calculate the partial derivative of Q along with w. Q is rewritten as

$$Q = |\frac{(jw+1)(jw+4)\Delta}{(jw+3)(jw+4)+6\Delta}| = |\frac{(4-w^2)\Delta+5w\Delta j}{(12+6\Delta-w^2)+7wj}|$$

We analyze the cost function, micro-fault, and frequency simultaneously; the general relationship is shown in Fig.7.

Its two-dimensional Bode diagram can be seen in Fig.8:

In Fig.8, the red line represents the amplitude-frequency characteristic curve of the cost function. From Figs.7 and 8,

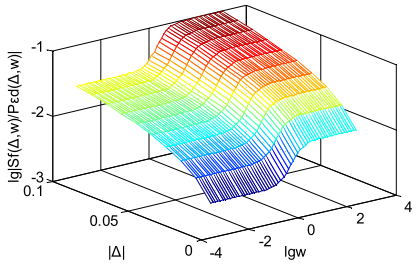

FIGURE 7. 3-D bode plot of cost function based on little fault.

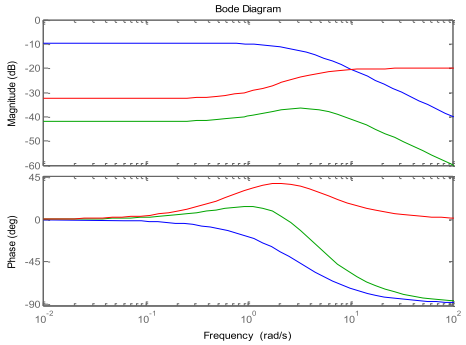

FIGURE 8. 2-D bode plot of cost function based on little fault.

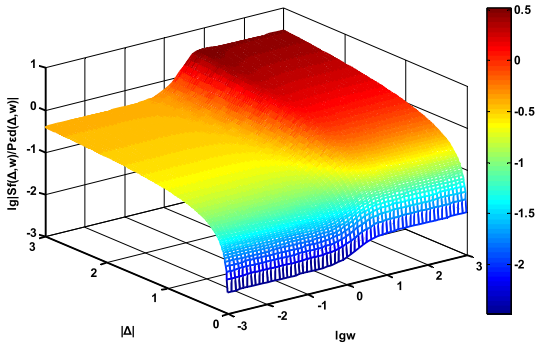

FIGURE 9. 3-D bode plot of cost function.

it can be observed that the trend graph of the cost function with respect to frequency is not obvious when the fault value is particularly small. However, it can be seen that the general range where the amplitude tends to be stable; therefore, the initial value of the frequency can be roughly determined to calculate the frequency using the gradient descent method, where the cost function probably reaches the extreme point.

In this study, the initial value of the frequency was as $5rad/s$, and the step length was set as 0.1. Referring to Eq.(32),.

$$\omega_{k+1} = \omega_k + \alpha' \frac{\partial |J_\omega|}{\partial \omega}$$

When a certain value was substituted, the value of the required frequency ω was $12.4rad/s$. To verify the correctness of the resonance thought, we enlarged the fault value range, as shown in Fig.10.

Define

$$Q = |\frac{(s+1)(s+4)\Delta}{(s+3)(s+4)+6\Delta}|$$

To obtain the value of the frequency w when the cost function Q is maximum, set $s = jw$ and transfer the problem to calculate the partial derivative of Q along with w. Q is rewritten as

$$Q = |\frac{(jw+1)(jw+4)\Delta}{(jw+3)(jw+4)+6\Delta}| = |\frac{(4-w^2)\Delta+5w\Delta j}{(12+6\Delta-w^2)+7wj}|$$

And then we can get that

$$\frac{\partial Q}{\partial w} = \frac{\partial |\frac{(4-w^2)\Delta+5w\Delta j}{(12+6\Delta-w^2)+7wj}|}{\partial w} = \frac{\partial (\frac{|\Delta|\sqrt{(4-w^2)^2+(5w)^2}}{\sqrt{(12+6\Delta-w^2)+(7w)^2}})}{\partial w} = 0$$

In this study, the example was set as $a = 1$, $b = 1$, $c = 1$, $m = -3$, $n = -4$. When fault Δ is a large accurate value, we can calculate the accurate value of the frequency w. For example,

$$\Delta = 1 \Rightarrow w = 12.7rad/s$$

As can be seen from Fig.9, with an increase in the fault value, the logarithm of the objective function will have an

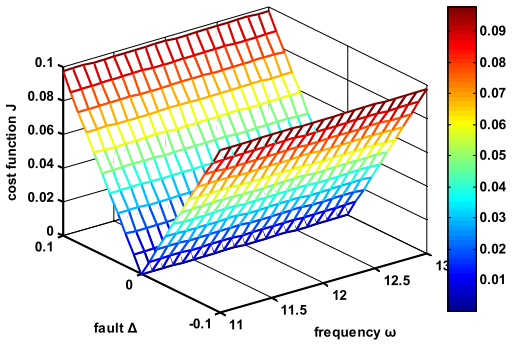

FIGURE 10. The amplitude of the cost function with different frequency.

extreme value, and when the fault value is small, the frequency corresponding to the occurrence position is close to the frequency value of the function when the target value is nearly smooth and tends to progress, as shown in Fig.7.

From the above results, the following conclusions can be drawn. For a significant fault, the resonant frequency can be directly calculated. For a small fault, because the cost function has no extreme point, the gradient optimization algorithm can be used to calculate the resonance frequency of the general value. According to Fig.7, the amplitude of the cost function has no extreme points. Therefore, the frequency that is designed to detect minor faults will have more selections. Here, we cause the frequency obtained by the gradient optimization algorithm to fluctuate within a certain range. When a minor fault occurs, the amplitude change in the cost function is, as shown in Fig.10 and Table. 2. In this study, the minor fault definition field was [0.01, 0.1].

From the above numerical comparison, we can see that when the frequency fluctuation is small, the change in the amplitude of the cost function is very small. This means that, for the detection of minor faults, the frequency selection of the auxiliary input signal is not limited to one value, which provides more possibilities for auxiliary input designs for minor fault detection.

B. AUXILIARY INPUT SIGNAL AMPLITUDE λ CALCULATION

In this section, amplitude λ is calculated in detail. The observe output of normal system $H = 20$, in the industry, 90% confidence intervals are generally used as the acceptable

TABLE 3. The comparison of the cost function amplitude.

J	ω=12 *rad/s*	ω=12.2 *rad/s*	ω=12.4 *rad/s*	ω=12.6 *rad/s*	ω=12.8 *rad/s*	ω=13 *rad/s*
Δ=0.01	0.0097	0.0097	0.0098	0.0098	0.0098	0.0098
Δ=0.03	0.0292	0.02932	0.0293	0.0293	0.0293	0.0293
Δ=0.05	0.0488	0.0488	0.0488	0.0489	0.0489	0.0489
Δ=0.07	0.0683	0.0684	0.0684	0.0684	0.0685	0.0685
Δ=0.09	0.0879	0.0879	0.0880	0.0881	0.0881	0.0882

space for the quality of the confidence space, to ensure the safety and reliability of the system is the main prerequisite for the design of AFD, the upper bound ΔH_1 of the system output is defined as $10\%H$. The threshold of the cumulative signal is designed as a fault decision standard. In this study, the cumulative signal δ is interrelated to the system residual and output, and in order to detect the fault quickly, the signal is designed as $\chi = 2.5\%H$, $t_d = 0.5s$, then we can obtain the following:

$$\left| \int_0^{t_d} |(\tilde{M}\frac{G_{eu}(\Delta)}{\tilde{V}-G_{yu}(\Delta)\tilde{U}} - \tilde{N}(\frac{G_{eu}(\Delta)}{\tilde{V}-G_{yu}(\Delta)\tilde{U}}\tilde{U}+1)\frac{1}{\tilde{V}})|\eta_t e^{jwt} d_t \right| \geq \chi$$

$$\left| \frac{G_{yu}(0)}{V - G_{yu}(0)U}\lambda \sin(\omega t_d) \right| \leq |\Delta H_1|$$

So the cost function can be written as

$$\begin{aligned} J_\lambda &= \lambda + \beta_1(P_{e\eta}(0)\eta_t - |\Delta H_1|) + \beta_2(\chi - \delta) \\ &= \lambda + \beta_1 \left(\left| L^{-1}\left(\frac{N}{VM - NU}\right) \right| \lambda \sin(\omega^* t_d) - |\Delta H_1| \right) \\ &\quad + \beta_2 \left(\chi - \left| \int_0^{t_d} \left| \frac{\tilde{M}G_{eu}(\Delta) - \tilde{N}}{\tilde{V} - G_{yu}(\Delta)\tilde{U}} \right| \lambda \sin(\omega^* t) e^{jw^* t} dt \right| \right) \\ &= \lambda + \beta_1(1.808\lambda - 0.5) + \beta_2(2 - 4.916\lambda) \end{aligned}$$

Setting the relaxation factors β_1 and β_2 as 0.5, the optimal amplitude λ can be calculated using the linear programming method, and the value is

$$\lambda = 0.267$$

and the auxiliary input signal is

$$\eta = 0.267sin\,(12.4t)$$

Then, the simulations are realized based on the design of the auxiliary signal, and conclusions can be drawn by analyzing the simulations.

C. ACTIVE FAULT DETECTION SIMULATION

The amplitude and frequency of the auxiliary input signal are designed and calculated using a practical case in the previous section with a certain faulty type. In this section, to verify the effectiveness of the designed auxiliary input signal for active fault detection, some simulations are performed based on the design of the auxiliary signal, and conclusions can be drawn through the simulation analysis. The case simulation is described as follows:

The faulty type is selected as in the above sections first, that is, $G_{yu}\,(\Delta) = G_{yu}\,(I + \Delta)$. The auxiliary input signal can be simulated by calculating the actual case as shown in Fig. 11.

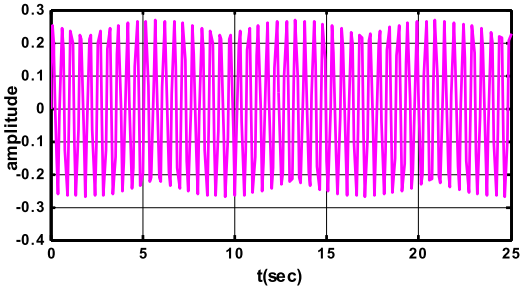

FIGURE 11. The auxiliary input signal.

As shown in Fig.12, the output of the system tracks the amplitude of the input signal r without a fault, and a small deviation can be observed after the fault occurs; however, in practice, external interference is unavoidable. A small deviation can often be ignored as noise; therefore, deviation is the key to active fault detection.

The residuals of the system and accumulation of residuals are shown in Fig.13 and 14. It can be observed that when the system fails, the small offset of the system's residuals is often ignored as noise as the system output. Then, by using the cumulative algorithm, the accumulated signal will exceed the threshold range, so a fault can be detected. This shows that the design of this method is feasible for realizing fault detection.

In this study, a specific fault-type system is considered as an example. It is proven that the active fault detection method based on an auxiliary input signal is preliminarily feasible. However, in practice, the type and size of faults are unknown. Therefore, in this study, we refer to Table. 1, we designed an auxiliary input signal with several faulty types, and the auxiliary input signal frequencies and amplitudes were optimized. Finally, a series of auxiliary input signals were combined and added to the system to verify the reliability of the active fault detection results.

TABLE 4. The frequency and amplitude of the auxiliary signal with diffferent faulty types.

faulty type	$S_f(\Delta)$	frequency range (rad/s)	the selected frequency (rad/s)	threshold χ	amplitude
$G_{yu}(I+\Delta)$	$\tilde{N}\Delta(I-U\tilde{N}\Delta)^{-1}M$	9.87-13.43	11.62	0.5	0.267
$G_{yu}+\Delta$	$\tilde{M}\Delta(I-U\tilde{M}\Delta)^{-1}M$	4.03-9.11	6.57	0.5	6.922
$G_{yu}(I+\Delta)^{-1}$	$-\tilde{N}\Delta(I+M\tilde{V}\Delta)^{-1}M$	2.90-3.15	3	0.01	4.46
$G_{yu}(I+\Delta G_{yu})^{-1}$	$-\tilde{N}\Delta(I+N\tilde{V}\Delta)^{-1}N$	0.03-0.32	0.18	0.01	1.07

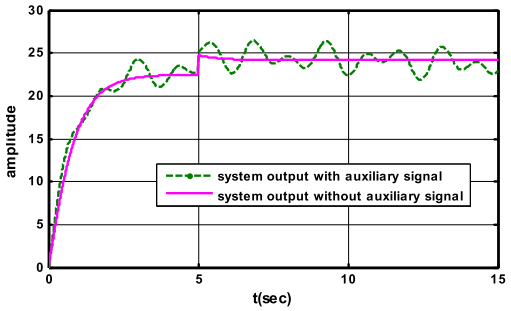

FIGURE 12. The system output signal.

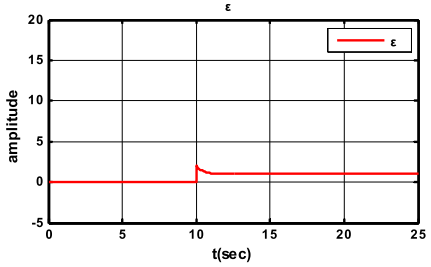

FIGURE 13. The system residual ε.

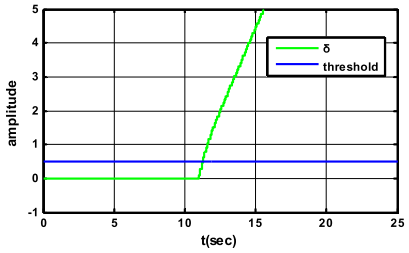

FIGURE 14. The CUSUM of the system residual.

Because the size of the minor fault is defined in a range, the obtained frequency is also within that range. However, according to Fig.10 and Table 3, the fluctuation in the obtained frequency value has little effect on the amplitude of the objective function. Here, we find the frequency of the average to be the selected frequency for subsequent simulations.

Remark 2: Random resonance low-frequency scanning is a great breakthrough in the detection of weak signals and has a wide range of applications. Detection of minor faults

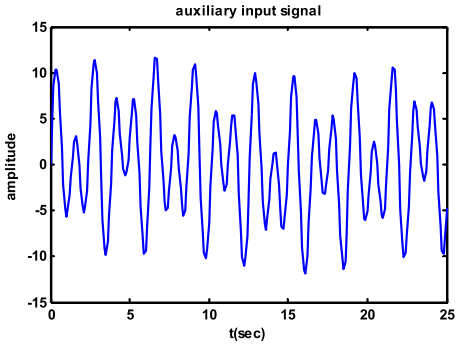

FIGURE 15. The integrated auxiliary input signal.

is one of the most representative applications. However, this method requires multiple frequency segments to be scanned individually to achieve detection and reduce the detection rate. To compensate for the shortcomings of the speed in detecting small signals with resonant low-frequency scanning, a sinusoidal excitation signal with a fixed frequency was proposed. The design of this signal considers the internal frequency changes of the system when multiple types of faults occur and realizes the fast and accurate detection of minor faults. At the same time, based on modern control theory, it ensures the internal stabilization of the parametric model of the system.

According to Table. 3, the frequency is designed as a fixed value when the faulty type is known, and four different auxiliary input signals are obtained with the four faulty types. The detection method was verified to be feasible because the actual failure is unknown, and the auxiliary signal designed for a single fault type may not detect all types of faults. Therefore, we designed excitation signals for each type of fault, and the composition of the integrated signal was used for unknown fault detection. Subsequently, a detection proposal is proposed. The auxiliary input signal was a combination signal, which was a new integrated excitation signal $\eta = \eta_1+\eta_2+\eta_3+\eta_4$ as shown in Fig.15. where the auxiliary input signals are $\eta_1 = 0.267sin(11.62t)$, $\eta_2 = 6.922sin(6.57t)$, $\eta_3 = 4.46sin(3t)$, $\eta_4 = 1.07sin(0.18t)$. We test the detection rate as follows:

First, when the system has no faults, the system residual and the accumulation of the residual will have negligible changes, see as Fig.16-17.

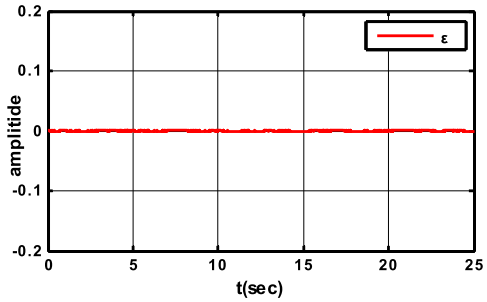

FIGURE 16. The system residual ε.

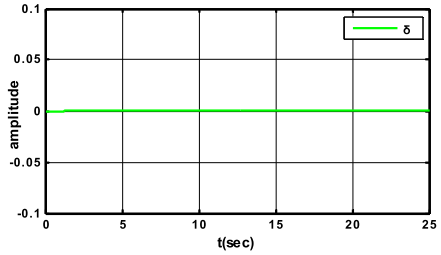

FIGURE 17. The accumulation residual δ.

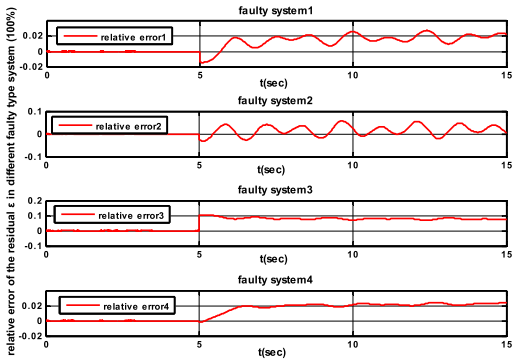

FIGURE 18. The relative error of system residual ε with different faulty type.

The auxiliary signal is input to the faulty system and fault detection is performed. The trends of the system residual relative error and the accumulation residual are shown in Fig.18-19. The system residual relative error is defined as $|\varepsilon_1 - \varepsilon_0|/\varepsilon_0$, and ε_1 and ε_0 are the system residuals when the fault occurs and when it does not, respectively.

In Fig.18 and 19, signals δ_1, δ_2, δ_3, and δ_4 in Fig.19 are the accumulation residual signals with different faulty systems. When faults occur, the change in the residual has little effect on the stability of the system, but the accumulation residual quickly exceeds the threshold such that the fault detection time is short. Therefore, active fault detection based on an auxiliary input signal design is a feasible method according in Fig.18-19.

Different types of faults can be detected when auxiliary input signals are combined. It has been demonstrated that the proposal is feasible, but the dominant role of the corresponding excitation signal has not been verified; in other words, the impact of other auxiliary signals on the current failure needs to be tested. To verify this effect, we selected two faulty

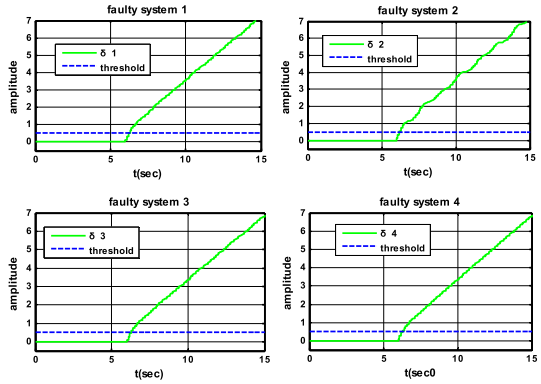

FIGURE 19. The accumulation residual δ with different faulty type.

systems as

$$\text{System I:}\quad G_{yu}(\Delta) = G_{yu}(I + \Delta)$$
$$\text{System II:}\quad G_{yu}(\Delta) = G_{yu}(I + \Delta)^{-1}$$

Then the simulations are drawn in Fig.20-21.

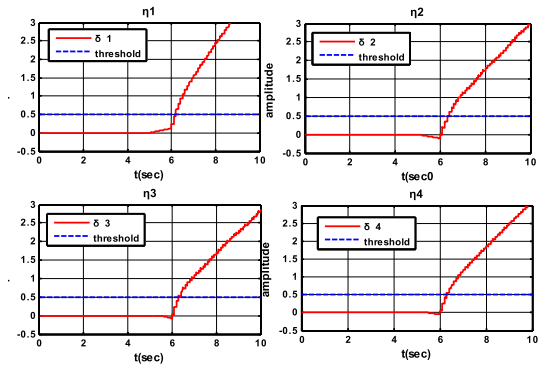

FIGURE 20. The accumulation residual δ of system I with different auxiliary input signal.

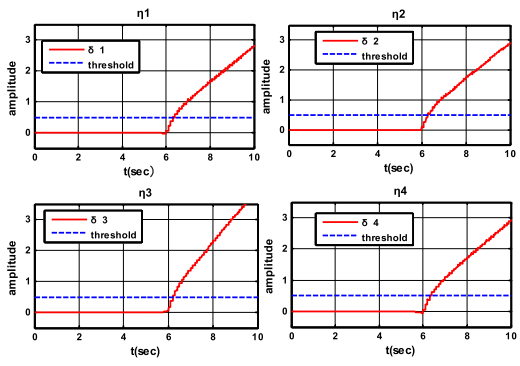

FIGURE 21. The accumulation residual δ of system II with different auxiliary input signal.

where the auxiliary input signals are $\eta_1 = 0.267sin(11.62t)$, $\eta_2 = 6.922sin(6.57t)$, $\eta_3 = 4.46sin(3t)$, $\eta_4 = 1.07sin(0.18t)$. As can be seen from the simulation results, when no fault occurs, the residual accumulation and signals are always zero, indicating that the addition of auxiliary input signals does not affect normal system operation. However,

TABLE 5. The fault detection time of different system with different auxiliary signal.

Faulty type	The time of fault occurs	The combined auxiliary signal	η_1	η_2	η_3	η_4
$G_{yu}(I+\Delta)$	5s	6.23s	6.09s	6.34s	6.41s	6.49s
$G_{yu}(I+\Delta)^{-1}$	5s	6.21s	6.39s	6.26s	6.12s	6.37s

under different minor fault conditions, after the addition of designed auxiliary input signals, the system residuals accumulation and signals can quickly exceed the set threshold in a short time, so as to achieve the condition of fault judgment. According to the data in Table. 5, the auxiliary signal designed for a certain type of fault has a faster detection speed and a good detection effect on faulty system. Thus, the method of designing the auxiliary signal and the method of injecting it into the system were verified.

Remark 3:

1. The integrated excitation signal is slightly slower for fault detection, but this signal can detect the minor faults successfully.

2. In our examples, four designed independent excitation signals can detect fault systems 1 and 2; however, they are not equal to all faulty types that can be detected with only a single excitation signal. This is because our design goal is to maximize the objective function, and the non-maximized objective function of the frequency may not be able to properly detect a fault. To ensure that fault detection is successful, the required excitation signal should contain the maximum frequency of the fault type.

3. In this paper, a first-order system with universal significance is selected as the simulation case, and sinusoidal auxiliary input signals for different fault types are designed to verify the feasibility of the active fault detection method proposed in this paper, and the fast effectiveness of AFD is illustrated in the simulation part. In the future, this method will be used to verify the feasibility of the complex system, and the actual system will be selected for modeling to realize the simulation of active fault detection.

V. CONCLUSION

The main idea of the active fault detection method based on auxiliary input signal design is that when a minor fault occurs, fault detection is aimed at maintaining the stability of the system. In other words, the stability of the system was not affected by the detection module. In this study, we designed the decision signal to determine the fault and used the cumulative sum method. When a fault occurs, the accumulation of the decision signal exceeds the threshold range of the design to judge system failure. In this method, the auxiliary input signal is set to a sinusoidal model; therefore, it is only necessary to design the amplitude and frequency of the auxiliary input signal.

First, the basic research framework is designed as a Youla parameterization framework, and then the frequency characteristics of the known fault feature matrix S_f. Based on this feature, the design objective function is set, and the fault feature matrix is the key to the design idea of the AFD. Then, the amplitude and frequency of the auxiliary input signal can be designed based on the cost function, and are calculated using the gradient descent method and linear programming algorithm, respectively. The design idea of the frequency is based on the thought of random resonance of minor fault detection, in which the frequency is designed as a fixed value in connection with a certain type and size fault. Therefore, we designed a series of auxiliary input signals with a certain frequency for each type of faulty system and then combined them to inject a system with an unknown fault to detect the fault. Finally, we select an actual simple first-order system example to describe the calculation of the optimal frequency and amplitude of the auxiliary input signal. To detect as many types of failure as possible, we designed a series of auxiliary signals and combined them into an integrated signal to be injected into the system. The simulation results demonstrated that the design idea is of practical significance.

In the case simulation stage of the auxiliary input signal proposed in this paper, a representative first-order system of general significance is selected. According to the fault characteristic matrix Sf of various minor fault systems, the corresponding internal frequency of the fault system is obtained, so as to design the corresponding frequency of the auxiliary input signal. Simulation results show that this method is fast and effective in detecting minor faults. The research focus of this paper is the research of auxiliary input signal, and the next research focus will be transferred to the application of this method. At present, there are corresponding studies in the chemical industry process and wind power generation, and corresponding achievements have been made in the mathematical modeling of the system. Since then, the research focuses on the design of auxiliary input signals for complex and high-level systems, and finally realizes the corresponding simulation of micro fault detection, further verifying the effectiveness of the proposed method, so as to explore more practical project fault detection technology and the combination of this method.

REFERENCES

[1] J. Wang, J. Zhang, B. Qu, H. Wu, and J. Zhou, "Unified architecture of active fault detection and partial active fault-tolerant control for incipient faults," *IEEE Trans. Syst., Man, Cybern. Syst.*, vol. 47, no. 7, pp. 1688–1700, Jul. 2017.

[2] W. Wu, Y. Kang, and L. Yao, "Learning observer based fault diagnosis and fault tolerant control for manipulators with sensor fault," in *Proc. CAA Symp. Fault Detection, Supervision Saf. Tech. Processes (SAFEPROCESS)*, Jul. 201, pp. 53–58.

[3] K. Huang, L. Cao, D. Wang, Q. Wang, J. Xu, and X. Zeng, "Impact of resistive-type superconducting fault current limiter on dynamics of VSC-MTDC systems," in *Proc. 5th Asia Conf. Power Electr. Eng. (ACPEE)*, Jun. 2020, pp. 1686–1691.

[4] A. Nra, R. Zarghami, R. S. Gharebagh, and N. Mostoufi, "A data-driven fault detection and diagnosis by NSGAII-t-SNE and clustering methods in the chemical process industry," *Comput. Aided Chem. Eng.*, vol. 49, pp. 1447–1452, Jan. 2022.

[5] H. Dai, K. Chen, Y. Wang, and H. Yu, "Fault detection method of secondary sound source in ANC system based on impedance characteristics," *J. Northwestern Polytechnical Univ.*, vol. 40, no. 6, pp. 1242–1249, Dec. 2022.

[6] Q. S. Imran, N. A. Siddiqui, A. H. A. Latiff, Y. Bashir, M. Khan, K. Qureshi, A. A.-S. Al-Masgari, N. Ahmed, and M. Jamil, "Automated fault detection and extraction under gas chimneys using hybrid discontinuity attributes," *Appl. Sci.*, vol. 11, no. 16, p. 7218, Aug. 2021.

[7] R. Nikoukhah and S. L. Campbell, "Auxiliary signal design for active failure detection in uncertain linear systems with a priori information," *Automatica*, vol. 42, no. 2, pp. 219–228, Feb. 2006.

[8] R. Nikoukhah, S. L. Campbell, and K. Drake, "An active approach for detection of incipient faults," *Int. J. Syst. Sci.*, vol. 41, no. 2, pp. 241–257, Feb. 2010.

[9] H. Niemann, "A setup for active fault diagnosis," *IEEE Trans. Autom. Control*, vol. 51, no. 9, pp. 1572–1578, Sep. 2006.

[10] H. Niemann and N. K. Poulsen, "Active fault detection in MIMO systems," in *Proc. Amer. Control Conf.*, Portland, Oregon, Jun. 2014, pp. 1980–1985.

[11] M. Simandl and I. Puncachaf, "Active fault detection and control: Unified formulation and optimal design," *Automatica*, vol. 45, pp. 2052–2059, Sep. 2009.

[12] J. Pan, F. Zhang, P. Li, Y. Tang, Y. Gu, and L. Shang, "Incipient fault detection based on Kolmogorov–Smironv test," in *Proc. 34th China Conf. Control Decis. Making*, 2022, pp. 566–571.

[13] J. He, B. Q. Yang, and Z. Wang, "On-line fault diagnosis and fault-tolerant operation of modular multilevel converters—A comprehensive review," *J. Elect. Mach. Syst.*, vol. 4, no. 4, p. 13, 2020.

[14] I. Punčochář, J. Široký, and M. Šimandl, "Constrained active fault detection and control," *IEEE Trans. Autom. Control*, vol. 60, no. 1, pp. 253–258, Jan. 2015.

[15] H. Niemann, "Dual Youla parameterisation," *IEE Proc. Control Theory Appl.*, vol. 150, no. 5, pp. 493–497, Sep. 2003.

[16] J. K. Scott, R. Findeisen, R. D. Braatz, and D. M. Raimondo, "Input design for guaranteed fault diagnosis using zonotopes," *Automatica*, vol. 50, no. 6, pp. 1580–1589, Jun. 2014.

[17] J. Możaryn, K. Bogusz, and S. Juszczynski, "Development of PLC based fault isolation and remote IIoT monitoring of three tank system," *IFAC-PapersOnLine*, vol. 55, no. 6, pp. 175–180, 2022.

[18] M. MaIga, N. Ramdani, and L. Trave-Massuyes, "Robust fault detection in hybrid systems using set-membership parameter estimation," *IFAC-PapersOnLine*, vol. 48, no. 21, pp. 296–301, 2015.

[19] C. Jauberthie, N. Verdière, and L. Travé-Massuyès, "Fault detection and identification relying on set-membership identifiability," *Annu. Rev. Control*, vol. 37, no. 1, pp. 129–136, Apr. 2013.

[20] L. Li, H. Zhang, J. Zhang, and X. Ren, "A new adaptive identification framework for nonlinear multi-input multi-output systems under colored noise," *Appl. Math. Model.*, vol. 103, pp. 105–121, Mar. 2022.

[21] A. Guarneros, I. Salgado, and I. Chairez, "Unsupervised learning for a clustering algorithm based on ellipsoidal calculus," in *Proc. 7th Int. Conf. Control, Decis. Inf. Technol. (CoDIT)*, Jun. 2020, pp. 1–9.

[22] A. E. Ashari, R. Nikoukhah, and S. L. Campbell, "Active robust fault detection in closed-loop systems: Quadratic optimization approach," *IEEE Trans. Autom. Control*, vol. 57, no. 10, pp. 2532–2544, Oct. 2012.

[23] H. Niemann, "Active fault diagnosis in closed-loop uncertain systems," *Fault Detection Supervision Saf. Tech. Processes*, vol. 38, no. 1, pp. 587–592, 2005.

[24] M. Mou and X. Zhao, "Incipient fault detection and diagnosis of nonlinear industrial process with missing data," *J. Taiwan Inst. Chem. Eng.*, vol. 132, Mar. 2022, Art. no. 104115.

[25] H. Wu, B. Zhang, and N. Liu, "Self-adaptive denoising net: Self-supervised learning for seismic migration artifacts and random noise attenuation," *J. Petroleum Sci. Eng.*, vol. 214, Jul. 2022, Art. no. 110431.

[26] Y. Sun, Y. Cao, H. Liu, W. Yang, and S. Su, "Condition monitoring and fault diagnosis strategy of railway point machines using vibration signals," *Transp. Saf. Environ.*, vol. 5, no. 2, Mar. 2023.

[27] L.-F. He, Q.-L. Liu, and Z.-J. Jiang, "Combined underdamped bistatic stochastic resonance for weak signal detection and fault diagnosis under wavelet transform," *Fluctuation Noise Lett.*, vol. 22, no. 1, pp. 1793–6780, Feb. 2023.

JINGJING ZHANG received the B.S. degree in automation and the master's degree in control science and engineering from the Beijing University of Chemical Technology, in 2014 and 2017, respectively.

Since 2017, she has been a Lecturer with the College of Electrical Engineering, Hebei University of Architecture, Zhangjiakou, China. Her research interests include the application of advanced control schemes to nonlinear, multivariable, and constrained industrial processes; modeling, optimization, and control for complex industrial process; nonlinear model-based control of polymer microscopic quality in chemical reactor; process monitoring; and fault diagnosis for complex industrial process.

LIMING LIU received the master's degree in control science and engineering from the Beijing University of Chemical Technology, in 2017.

He is currently an Electrical Engineer with Zhangjiakou Sany Wind Power Technology Company Ltd., mainly researching intelligent manufacturing technologies.

LEI WANG received the M.S. degree.

He is currently with the Hebei University of Architecture, Zhangjiakou, China. His research interests include image processing and deep learning.

FEIFAN YANG is currently pursuing the degree in mechanical design intelligent manufacturing automation with the Hebei University of Architecture, Zhangjiakou, China.